PCCP

PAPER

View Article Online
View Journal | View Issue

Cite this: *Phys. Chem. Chem. Phys.*, 2015, **17**, 26198

Dynamic interface tension of a smectic liquid crystal in anionic surfactant solutions

Kirsten Harth,*[a] Larissa M. Shepherd,[b] James Honaker[c] and Ralf Stannarius[a]

Received 17th July 2015,
Accepted 8th September 2015

DOI: 10.1039/c5cp04193g

www.rsc.org/pccp

The interface tension of a smectic liquid crystal with respect to a surrounding ionic surfactant solution is investigated at concentrations above and below the critical micelle concentration (cmc). A simple measurement technique has been developed recently [*Phys. Chem. Chem. Phys.*, 2013, **15**, 7204], based on the geometrical analysis of the shape of smectic bubbles in water that are deformed by the buoyancy of trapped air bubbles. After preparation of the smectic membranes in the solution, we measure both the time dependence of their dynamic interface tension as well as the asymptotically reached static tension values. These are established about 15 minutes after the membrane preparation. At large enough concentrations of the surfactant (above the critical micelle concentration), the interface tension drops to 6 mN m^{-1}. At the lowest possible surfactant concentrations in our experiment, the equilibrium tension reaches 20 mN m^{-1}, which is almost equal to the smectic surface tension respective to air. The tension of a freshly drawn film exceeds this value by far.

1 Introduction

Thermotropic liquid crystals (LC) are a peculiar class of fluids characterized by molecular orientational order. Smectic phases additionally possess one or higher-dimensional positional order. These structural features are the reason for the appearance of characteristic properties like optical birefringence and anisotropic elasticity that are usually found in solids only. Such properties are accompanied by fluidity of the material. This combination qualifies LCs in a unique way for technical applications, *e.g.* in displays, but also as a objects for fundamental physical research.

The interplay between geometrical restrictions and elasticity has moved into focus of scientific interest in recent years, as a fundamental prerequisite for the design of novel functional and metamaterials. An interesting aspect is the investigation submillimeter-sized shells of ordered fluid materials.[1–4] Such structures can be produced *e.g.* using microfluidic co-flow techniques.[5] A droplet of an isotropic fluid wrapped in a film of LC material is embedded in another isotropic fluid. Polymers or surfactants are added to the inner and outer liquid for stabilization of the shell-structure, as well as for the orientation of the mesogens at the interface to the solution. Such shells are usually produced in the higher temperature isotropic phase of the mesogenic material, and thereafter investigated in the nematic phase. Surface stabilization is crucial in such shells, as the nematic phase possesses no internal molecular layer structure to stabilize the thin films.

Smectic shells, that exhibit layers with an orientation depending on the anchoring conditions of the material at the interfaces, are less intensively investigated. When the anchoring of the LC at the water interface is homeotropic (average mesogen orientation perpendicular to the interface), the smectic layers are parallel to the interface, at least in sufficiently thin films (thicknesses up to a few μm). In that case, the smectic film will be additionally stabilized by the molecular layer structure, and even a preparation of stable centimeter-sized bubbles is possible. Homeotropic anchoring can be induced, *e.g.*, by surfactants like sodium dodecyl sulfonate (SDS) or sodium dodecyl benzene sulfonate (SDBS, LAS). Such centimeter-sized bubbles have been reported earlier.[6,7] Anchoring transitions induced by surfactants can be useful in chemical or biological sensors.[8]

While surface tensions of several liquid crystal phases with respect to air have been studied extensively see, *e.g.* ref. 9–14, reports of interface tensions of smectics with respect to aqueous environments are rather scarce. Kim *et al.*[15] have measured the interface tension of the nematic 5CB using the pendant droplet method and obtained values of 1.5 mN m^{-1} or 7 mN m^{-1}, depending on which data for the liquid crystal density were used. The problem with their experiment is the small density difference between the LC droplet and the surrounding surfactant solution. Kim *et al.* had added the cationic surfactant cetyl trimethylammonium bromide (CTAB) to the water. With pure water, the

[a] *Institute of Experimental Physics, Otto von Guericke University Magdeburg, D-39106 Magdeburg, Germany. E-mail: kirsten.harth@ovgu.de; Fax: +49 391 67 18108; Tel: +49 391 67 58169*
[b] *Department of Fiber Science & Apparel Design, Cornell University, Ithaca, New York, USA*
[c] *Liquid Crystal Institute, Kent State University, Kent, Ohio, USA*

LC drop shape was practically indistinguishable from a sphere. From this, one may infer that the interface tension to pure water is much larger than in presence of a surfactant. A quantitative value, however, could not be determined. Gharbi *et al.*[16] measured the interface tension of nematic 5CB to a mixture of water, $CaCl_2$ and polyvinyl alcohol. They found a value of 5.6 mN m^{-1} for the planar anchoring conditions in this environment. For 5CB to pure water, Proust *et al.*[17] had reported a value of 26 mN m^{-1}, again with planar alignment. Even less is known about smectic interface tensions to other fluids. A value of $\approx$33 mN m^{-1} can be estimated from the shape of picoliter droplets of an aqueous solution of 5% ethylene glycol[18] on a freely suspended smectic A film.

A recently introduced method allows the simple and exact measurement of interface tensions of smectic LCs in a surrounding liquid.[7] Instead of the very small buoyancy of a smectic droplet in water, the buoyancy of a millimeter-sized air bubble trapped beneath the membrane induces an easily measurable membrane deformation. The method depends on the possibility to prepare a smectic film in the surfactant solution or pure water, and trapping of an air bubble. We employ this method to measure the static and dynamic LC interface tensions in anionic surfactant solutions. We address the adsorption of the surfactant to quiescent bubbles at concentrations below the cmc. Equilibrium interface tensions at various surfactant concentrations are reported.

The surfactant adsorption dynamics take place on the time scale of several minutes until an equilibrium coverage is reached. These timescales may substantially influence the stability of freshly formed LC shells, where surfactant concentrations of few percent in weight are commonly used. The time-scale of surfactant adsorption at an LC interface as well as the flow field around the shell set the limiting conditions.

The adsorption of surfactants to fluid–fluid interfaces of isotropic fluids has been a permanent topic of research for almost 100 years. Fluid–fluid interfaces were first addressed in the 1940's by Alexander[19] and Ward and Tordai.[20] The tension of an interface of a fluid to a surfactant solution is determined by its coverage with surfactant molecules. When the solution is saturated and in equilibrium with the interface, the surface coverage is referred to as complete. The lowest concentration at which this occurs is usually referred to as the critical micelle concentration (cmc). Adding more surfactant to the solution only leads to the formation of additional micelles in the solution. The interface tension can be assumed to be almost independent of surfactant concentration above the cmc. Small decreasing or increasing trends may be possible.[21] Below the cmc, the surface coverage remains incomplete even in equilibrium, and the interface tension increases with decreasing surfactant concentration. Interfacial tension and area coverage are usually interrelated by adsorption isotherms, the most frequently used ones are the Langmuir and Frumkin isotherms. Direct measurements of the area coverage have been achieved, *e.g.* by ellipsometry, infrared spectroscopy or neutron reflectometry.[22–25] The agreement of the heuristic models with the few available data is often not satisfactory.[21,26] We will therefore not attempt any conversion of our measured interface tension data to area coverages. It is experimentally proven that the simple Gibbs equation of state is well applicable below, but also above, the cmc.[26] Here, we use it in a slightly modified form,[27]

$$\frac{\mathrm{d}\left(\gamma_0 - \gamma_{\mathrm{eq}}(c)\right)}{\mathrm{d}(\ln c)} = nk_{\mathrm{B}}T\Gamma, \qquad (1)$$

where γ_0 is the interface tension without surfactant, $\gamma_{\mathrm{eq}}(c)$ is the equilibrium value of the interface tension at a bulk surfactant concentration c, k_{B} is the Boltzmann constant, T the temperature and Γ the interface coverage. The value of $n = 1$ is adopted for nonionic surfactants, whereas $n = 2$ represents monovalent ionic surfactant when it is fully ionized at the interface. From this, we may expect a linear relation between $\gamma_0 - \gamma_{\mathrm{eq}}(c)$ and $\ln(c)$ below the cmc.

In addition to these equilibrium properties, the dynamic tensions during the establishment of this equilibrium are another important aspect. When an interface is freshly formed (or rinsed off all surfactant), the surfactant will adsorb over a time period of minutes, sometimes of hours. One has to discriminate between kinetic and diffusion limited adsorption models. The latter apply to most nonionic surfactants, in absence of adsorption–desorption barriers. A first general solution to this problem under the assumption of diffusion-limited adsorption was given by Ward and Tordai.[28] A final decrease of the interface tension with $\gamma(c, t) - \gamma_{\mathrm{eq}}(c) \propto t^{-1/2}$ was predicted and has been confirmed experimentally. The adsorption dynamics of ionic surfactants below the cmc differ strongly from those of nonionic surfactants, in that adsorption of the surfactant molecules at the interface builds up an electric double layer, acting as an adsorption barrier due to electrostatic repulsion. Bonfillon *et al.*[27] modeled the adsorption dynamics of ionic surfactants: at short times after preparation of the surface, electric field effects are negligible and the adsorption is diffusion-limited. At intermediate times, when the surface coverage Γ is still small, desorption is not yet relevant, but the electrostatic contributions increase. This leads to the formation of a plateau where Γ is proportional to $\ln(t)$ and the interface tension $\gamma(c, t)$ decreases only very slowly. Finally, when the surface coverage approaches its equilibrium value, the interface tension decreases linearly with time. Their theoretical predictions have been confirmed experimentally within the same publication for an SDS solution. Ritacco *et al.*[29] investigated the adsorption of the cationic surfactant DTAB and found similar behavior, but no plateaus occurred for concentrations $c < 0.5$ cmc. They fitted the late time decay to an exponential function $\gamma(c, t) - \gamma_{\mathrm{eq}}(c) \propto \exp(-t/\tau)$. By appropriately salting the solution, the electric double layer formation is inhibited and diffusion-limited kinetics are recovered, $\gamma(c, t) - \gamma_{\mathrm{eq}}(c) \propto t^{-1/2}$. The tension of an initially bare droplet expanding at constant volume influx was investigated by MacLeod and Radke,[30] who also pointed out a significant difference when the surfactant was dissolved in the gas, fluid or both phases.

SDS and SDBS, used for the LC shells in ref. 31 and 32, are typical examples of anionic surfactants. Whereas SDS provides a more rigid anchoring of the LC director at the surface,[32] a motivation to use SDBS is its solubility in larger concentrations in water–glycerol mixtures.

2 Experimental method

We prepare solutions of SDBS (Sigma Aldrich, technical grade) between 0.005 and 0.5 wt% in distilled water. The critical micelle concentration is between 0.065 wt%[33] and 0.1 wt%.[34] The concentration dependence of the equilibrium surface tension to air has been measured by Kumar *et al.*[33] In the range $c = [0.065...0.2]$ wt% (above the cmc) it follows a linear dependence, decreasing with 0.6 mN m^{-1} per 0.1 wt%. At 0.1 wt%, it assumes a value of 32.9 mN m^{-1}. For our highest concentrations of $c \approx 0.5$ wt%, extrapolation yields 30.5 mN m^{-1}, see ref. 7. Below the cmc, it strongly increases, at a concentration of 0.0135 wt% one finds 45.5 mN m^{-1}.

The surfactant induces homeotropic anchoring in nematic liquid crystals.[35] Homeotropic alignment is important for arranging the smectic layers parallel to the surface. Pure water yields planar anchoring and consequently a bookshelf geometry of smectic layers. Thus, we expect that below a certain surfactant concentration, no stable smectic films can be formed.

The liquid crystal studied is a 50 : 50 wt% mixture of two phenylpyrimidine derivatives, 2-(4-*n*-hexyloxyphenyl)-5-*n*-octyl-pyrimidine and 5-*n*-decyl-2-(4-*n*-octyloxy-phenyl)pyrimidine, with a broad smectic C range. The mesophase sequence is: smectic C 52 °C smectic A 68 °C nematic 72 °C isotropic. All experiments have been performed at room temperature where the material is in the smectic C phase (molecular director tilted respective to the layer normal). This phase can be supercooled well below 20 °C. The surface tension to air is γ_{air} = 22.45 mN m^{-1} at 25 °C.[36]

We use a setup similar to that described in ref. 7, it is sketched in Fig. 1. A transparent cuboid acrylic glass container is filled with a surfactant solution up to approx. 7 cm above its bottom. Near the center of the bottom plate, a coaxial double capillary dispenser is placed. The inner capillary is connected to a syringe providing the fluid inside the smectic bubble. Through the annular ring between outer and inner capillary, liquid crystalline material is supplied to form the bubble membrane. Small air bubbles can be injected into the inner tube by an air-filled syringe connected to the solution's tubing *via* a *t*-junction. Small air bubbles injected into this tube will be transported to the dispenser nozzle with the inner fluid. The top of the outer capillary is slightly flared to provide a larger support of the LC bubble, the outer diameter of the opening was approx. 2.3 mm. The inner capillary has a diameter of 1 mm and consists of steel. The syringes are operated manually using a screw mechanics. At low surfactant concentrations well below cmc, the smectic bubbles are quite susceptible to rupture, so that a steady and precise supply of the interior fluid is required. The bubble is illuminated with parallel light of a blue LED and observed in transmission with a Canon EOS 550D camera.

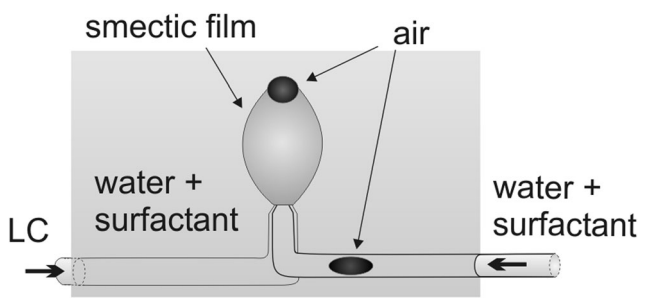

Fig. 1 Sketch of the experimental setup. The illumination and observation technique (power LED, lens and camera) are not shown. Images are taken in transmission.

The experiment proceeds as follows: a small amount of smectic material is supplied through the outer capillary until it forms a small, closed cap covering the opening. Then, surfactant solution is carefully pressed through the inner capillary to inflate a smectic bubble from cap material. When such a bubble has formed, we set the start time for the measurement. The bubble is then further inflated to a diameter between 0.5 and 2 cm, whereby an air bubble is injected. The air bubble rises to the top of the smectic bubble and causes a deformation that allows the determination of the smectic film tension. Images are taken until either the system appears to be equilibrated (no further shape changes), or until the smectic bubble pinches off. Then, a new experiment is prepared starting with a fresh smectic bubble. With our smectic C material, bubbles could be prepared down to surfactant concentrations of at least 0.005 wt%, but below a certain surfactant concentration it was impossible to inject an air bubble without rupture of the smectic film. The lowest surfactant concentration at which measurements were successful was 0.0135 wt%.

3 Calculating the interface tension

Two exemplary pictures are shown in Fig. 2. In transmission, the air bubbles appear dark due to refraction, except for a bright spot in the center. The air bubbles are found trapped in different geometries: in most cases at high surfactant concentrations, the smectic film holds the air bubble at a contact line above the air bubble equator (Fig. 2, left). This is a stable situation, because a further rise of the air bubble would lengthen the contact line, thereby increasing the capillary forces of the smectic film that counteract buoyancy. Another geometry is often encountered at low surfactant concentrations (Fig. 2, right). There, the larger part of the air bubble is above the contact line and the air bubble contour has a well-defined edge at that line.

The smectic film has two contact lines, one at the bottom capillary and one to the air bubble, and in equilibrium it forms a minimal surface with constant mean curvature (Delauney surface) between them. We can safely assume that the shape of the smectic bubble is permanently in a quasi-equilibrium during the measurements, and that it reflects a force balance at the momentary interface tension, except when a pinch-off occurs. In order to calculate the interface tension of the smectic film to the surrounding surfactant solutions, we need to measure the length πd_{ring} of the triple contact line at the air bubble, the angle θ of the smectic membrane to the vertical at the contact line (Fig. 3), the volume V_{air} of the air bubble, and

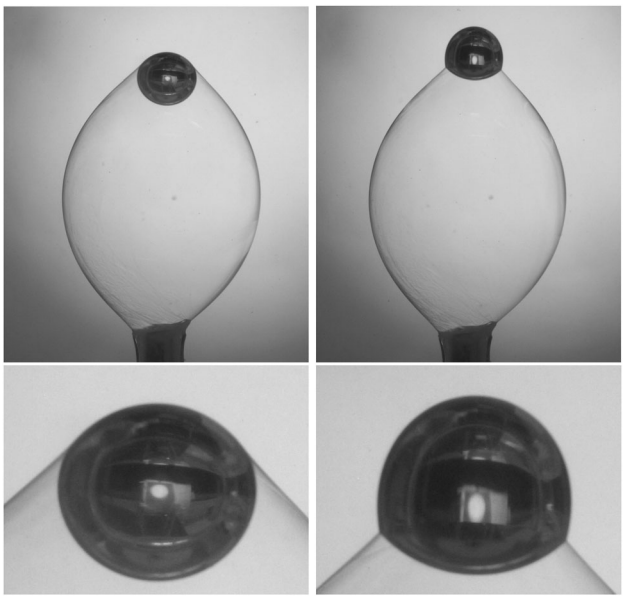

Fig. 2 Images of a smectic bubble with an entrapped air bubble in a 0.027% SDBS surfactant solution, well below the cmc. The sizes of the images in the top row are 13 mm × 15.2 mm. The bottom images are enlarged views of the air bubble. The air bubble volume corresponds to an equivalent diameter of 2.52 mm. Note the different attachment geometries of the air bubble to the smectic film. It started with an almost spherical air bubble (left image) where the kink at the line of contact is hardly resolved. This shape is typical for surfactant concentrations above the cmc. It is sometimes observed at intermediate concentrations below the cmc as well, where after some time, it transforms within few seconds to the geometry shown in the right image: the line of contact shifts below the air bubble equator and a clearly visible kink of the air bubble contour forms. At low surfactant concentrations ($c < 0.025$ wt%), the latter geometry is almost exclusively observed from the beginning. For the evaluation of the smectic film tension, these different air bubble configurations are not relevant, and will not be discussed further.

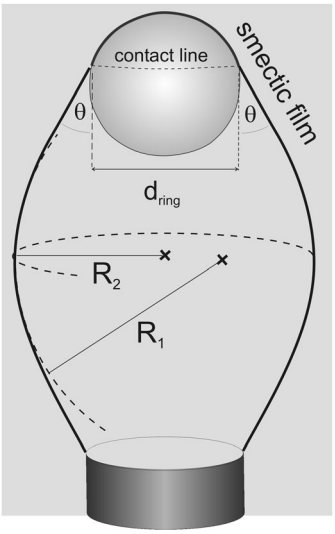

Fig. 3 Sketch of the smectic and air bubble geometries and definition of geometrical parameters.

the principal radii of curvature of the smectic bubble (R_1, R_2). The latter are needed to determine the Laplace pressure inside the smectic bubble from the mean curvature of the bubble surface. It adds a small correction to the buoyancy forces driving the air bubble upward. The interface tension is found from[7]

$$\gamma = \frac{V_{\mathrm{air}}(\rho - \rho_{\mathrm{air}})g}{2\pi d_{\mathrm{ring}}\left[\cos\theta - \frac{d_{\mathrm{ring}}}{4}\left(\frac{1}{R_1} + \frac{1}{R_2}\right)\right]} \qquad (2)$$

where ρ, ρ_{air} are the densities of the surfactant solution and the air, respectively, θ is defined in Fig. 3, and g is the gravitational acceleration.

These geometrical quantities are obtained from the raw images using a semi-automatic self-developed computer routine. The contact line of the air bubble to the smectic film apparently splits the image of the air bubble into an upper and a lower cap. In our previous study,[7] it was justified to approximate these regions by two sphere caps. In the present work, particularly at sub-cmc concentrations, we often had to cope with a different geometry of the air bubble, with the contact line below its equator (see Fig. 2, right). Then, the upper part of the bubble strongly deviates from sphere cap shape, which is a consequence of the hydrostatic pressure gradient along the vertical. It seems that the surface coverages at the smectic and air interfaces of the solution play a role in the air bubble geometry. In this study, the volume of entrapped air was determined from the evaluation of the complete air bubble contour. For a given set of dynamic tension measurements with the same bubble, the air volume V_{air} is constant. Then, the measured individual values in the series were averaged to obtain V_{air}. Within such sets, uncertainties in the determination of the air bubble volume do not affect relative surface tension values and time trends.

Apart from the air volume and length of the contact line, any details of the air bubble shapes are irrelevant for the presented interface tension measurements. The exact geometry of the air bubble is influenced by the (dynamic) smectic interface tension to the surfactant solution, the surface tension of the surfactant solution to air, and the surface tension of the smectic LC to air. The only force that can compensate the buoyancy and hold the air bubble in place are mediated by the smectic membrane.

All shape changes are slow and proceed on the time scale of tens of seconds (except during pinch-off, when too large air bubbles escape the smectic enclosure). Thus, the momentary membrane shapes can be considered as static and reflect equilibrium configurations for the momentary values of interface tensions.

The maximum size of an air bubble that can be held by the film can be estimated from the case when $\theta = 0$ (smectic film attaches vertically to the bubble, $d_{\mathrm{ring}} \approx d_{\mathrm{air}} \ll R_1, R_2$ by $d_{\max} \approx \sqrt{12\gamma/(\rho g)}$). The length of the bottom contact line of the smectic film at the meniscus to the capillary must be larger than this maximum air bubble circumference as well. Otherwise, the smectic bubble may pinch off near the bottom when it traps a large air bubble. As the dynamic interface tension between smectic and the solution initially tends to decrease with time, a bubble that is initially held by the film may escape the smectic bubble at later time due to the decrease in interface tension when the coverage with surfactant increases.

4 Equilibrium interface tensions

The first quantity of interest describing the smectic/solution interface is the asymptotically reached equilibrium value $\gamma_{eq}(c)$ of the interface tension. The time scale to achieve this stationary state is not known *a priori* and depends on the surfactant concentration. From literature (*e.g.* ref. 37) one may expect at least 10 minutes for the establishment of equilibrium. In our experiments, we wait until the bubble shapes remain constant for a sufficiently long time. As we will show below, a plateau in the interface tension is reached after $\approx$15 minutes. We do not exclude that further changes might occur for certain surfactant concentrations, as reported in literature for other interfaces,[27] but we found no evidence for that. Several test experiments have been performed over time periods of up to 60 minutes without an indication of any observable long-term changes of γ. Fig. 4 shows the measured equilibrium values γ_{eq} in dependence on the surfactant concentration. Each point represents an average of several individual measurements. The lower concentration limit was set by the ability to prepare smectic bubbles that are stable enough to trap air bubbles for measurements.

Measurements below the cmc performed with the same surfactant solution on different days were found to yield slightly different results, the interface tension values varied by up to $\pm$10%. On the other hand, there were no visible trends that could indicate some aging or deterioration of the solutions. In Fig. 6, these experimental fluctuations are evident in the range of low surfactant concentrations. We attribute them to the high sensitivity of the interface tension to some unidentified external influences below the cmc. Above the cmc, the variations of measured $\gamma_{eq}(c)$ were much lower.

5 Dynamic interface tensions

The measurement of the dynamic tension was performed as follows: the smectic bubble was prepared, a first photo was taken, which is used as reference for t = 0. Then an air bubble was inserted. Occasionally, an air bubble was already contained in the freshly drawn smectic bubble. After that, images were recorded in certain time intervals to record changes in the bubble geometry, the time intervals were registered with an accuracy of about 1 second. Fig. 5 shows the difference of the first and last images for 4 exemplary series at different concentrations. No shape changes are detectable for $c \geq 0.1$ wt%, *cf.* Fig. 5a. At concentrations $c \leq 0.05$ wt%, noticeable differences between the initial and final smectic bubble shapes occur. These indicate a time dependence of the interface tensions on a time scale of minutes.

Since the preparation of the smectic bubble is performed manually and takes at least 20 seconds, the initial time for the experiment is not set exactly. The volume growth rate of the smectic bubble was not recorded and a small initial adsorption during bubble preparation from the LC bulk cannot be excluded. The time axis refers to the end of the smectic bubble preparation process, so that the actual initial value $\gamma(t = 0)$ may be somewhat higher than extracted from the experiments, and the time axes of individual time evolutions may be shifted with respect to each other by up to 30 seconds. Nevertheless, we

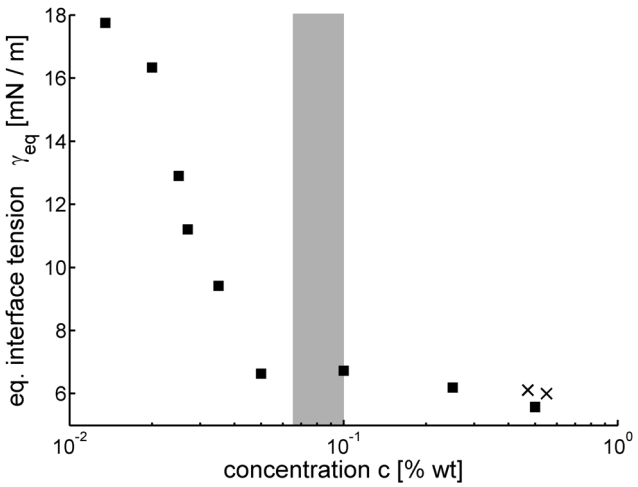

Fig. 4 Equilibrium interface tensions $\gamma_{eq}(c)$, the shaded region marks the range of critical micelle concentrations from ref. 33 and 34. The two crosses correspond to the measurements published in ref. 7.

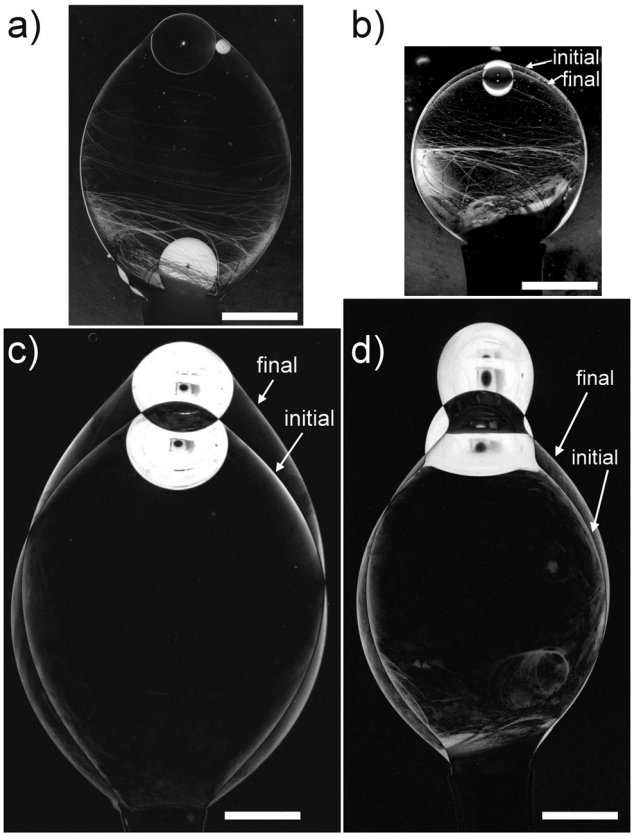

Fig. 5 Absolute difference images of initial and final ($t >$ 30 min) contours of the bubbles at concentrations of (a) 0.1 wt%, (b) 0.05 wt%, (c) 0.027 wt% and (d) 0.0135 wt%. The geometry is essentially constant in (a). An additional air bubble, not touching the smectic bubble, is situated near the capillary opening in the last image. The bubble in (d) pinches off later. The white network structures on the smectic bubbles are caused by migrating dislocations in the layer structure (film thickness steps). The scale is identical for all images, the bars represent 2 mm.

observe the same clear trends. For the slopes of the $\gamma(c, t)$ graphs (Fig. 6), this uncertainty of absolute time values is irrelevant. The characteristic times for the equilibration of the surfactant coverage are more than one order longer than temporal shifts related to the uncertainty of the starting point. For low surfactant concentrations, the experiment usually ends when the air bubble escapes from the smectic bubble. At the lowest concentration, the bottom cap of the air bubble is obscured by a meniscus before pinch-off, see Fig. 5d. In all other cases, we collect data until no geometric changes are detectable.

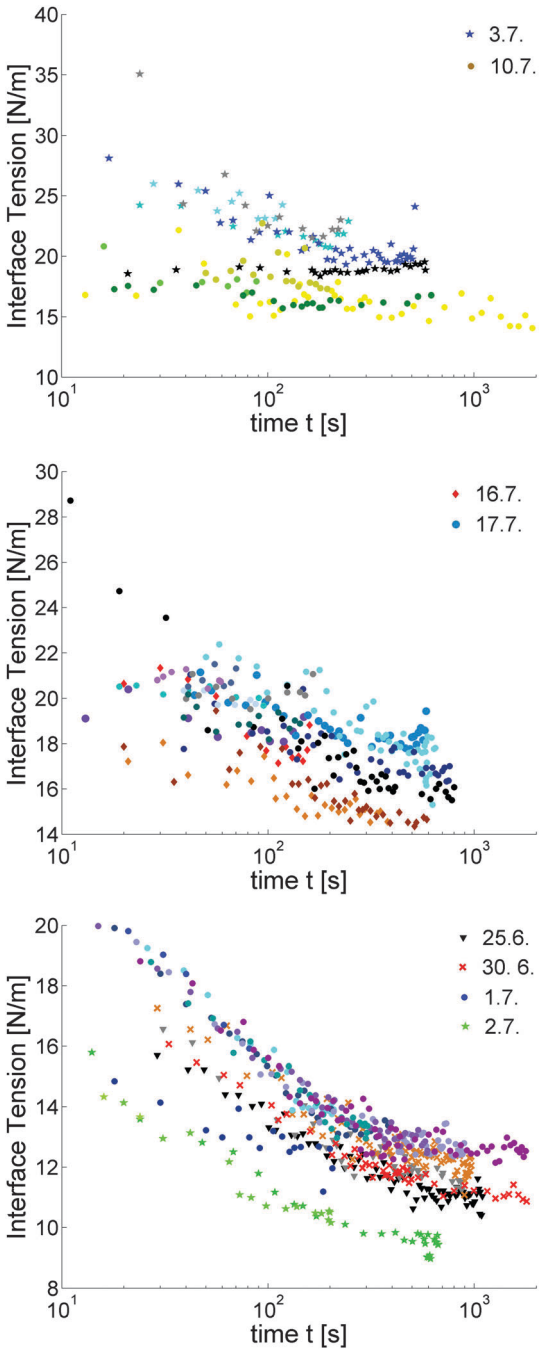

Fig. 6 Dynamic interface tensions $\gamma(t)$ for surfactant concentrations of 0.0135 wt%, 0.020 wt% and 0.027 wt% (top to bottom, respectively). Identical symbols correspond to measurements of the same day, different colors (greyscales) reflect different runs of the experiment.

Fig. 6 shows the evolution of the dynamic tensions for different surfactant concentrations. Several trends are evident: first, the initial values $\gamma(t = 0)$ for the lowest concentration c reach approximately 35 mN m^{-1}, and they decrease with increasing surfactant concentrations. We did not attempt to extrapolate these values to an actual initial value, since the experiment is not well adapted for that. However, the interface tension of the bare interface to water may be expected to be even larger. To our knowledge, there is only one reported value of an LC–water interface tension: $\gamma_{5CB} = 26$ mN m^{-1} for the nematic 5CB,[17] in the same order of magnitude. Second, the difference between the initial value and final value of $\gamma(c, t)$ increases with decreasing surfactant concentration c. Third, the decay rates slightly decrease with decreasing c. These are essentially determined by the electrostatic adsorption barriers.[27] This trend in decay rates is similar to previous observations of Bonfillon *et al.*[27] for SDS–water solutions to air and Ritacco *et al.*[29] for DTAB solutions to air.

Plateau values are reached after $\approx$15 min. In experiments where we recorded the bubbles for more than 30 minutes, no further changes of γ were evident. Individual runs are conveniently fitted by an exponential $(\gamma(c, t) - \gamma_{eq}) \propto \exp(-t/\tau)$ in the spirit of ref. 26 and 29, where τ and γ_{eq} are fit parameters. A discrimination between different functional dependencies[27,29] of the late time decays is impossible within the accuracy of our measurements, and was out of the scope of this paper. The diffusive adsorption regime and the formation of intermediate plateaus of $\gamma(t)$ in these works occurred for $t < 10$ s, a time range that is inaccessible with our simple setup. For SDBS solution/air interfaces of $c <$ cmc, no intermediate plateaus were observed by Phan *et al.*[38]

All experiments performed within the same day (up to a dozen within a few hours) gave very reproducible results, even though each time a different smectic film was prepared. But on the other hand, experiments with the same surfactant solution performed on different days showed deviations of up to $\pm$10% not only in the initial $\gamma(0)$, but also in the equilibrium values. This is particularly evident in the two long-term experiments in Fig. 6, bottom. If a sequence of experiments performed at successive days is compared, there is no systematic trend in the interface tension variation.

6 Conclusions and summary

Equilibrium interface tensions and the dynamic establishment of the equilibrium have been determined for a smectic liquid crystal material in thin film geometry in an aqueous surfactant solution. The anionic surfactant SDBS was studied in the range of sub-cmc concentrations. The lower concentration limit was on the order of 0.01 wt% of SDBS, for lower concentrations we could not produce stable smectic films with entrapped air bubbles. A reasonable explanation is that the SDBS is necessary to induce homeotropic anchoring of the smectic mesogens at

the LC–water interface, which leads to an arrangement of the smectic layers in the film plane and thus the stabilization of thin films. We assume that at lower concentrations of the surfactant, this anchoring is lost and the preferentially planar anchoring of the LC at pure water interfaces[17] takes over. In that case, smectic free-standing films are not stable. The smectic forms focal conics or bookshelf layer alignment depending on the film thickness.

Equilibrium interface tensions at $c \approx 0.5$ wt%, well above the cmc, have been reported earlier.[7] For $c >$ cmc, the interface tensions only slightly increases with decreasing surfactant concentration, by less than 1 mN m^{-1} between 0.05 wt% and 0.5 wt%. A similar trend was also observed by Kumar *et al.*[33] for the SDBS solution/air interface. Above the cmc, the SDBS adsorption to the LC/solution interface takes less time than the bubble preparation. No significant time dependence of the interfacial tension could be detected.

Below the cmc, the interface tension is time dependent. A plateau is reached after 15 min. The equilibrium interface tensions $\gamma_{eq}(c)$ are strongly concentration dependent. In the concentration range of $c \approx [0.02...0.05]$ wt%, it can be roughly approximated by an logarithmic dependence $\gamma_{eq} \approx [24.3 - 23.3 \log_{10}(c/\text{wt\%})]$ mN m^{-1} in accordance with eqn (2). In the measurements of the dynamic surface tensions, we find that the difference $\gamma(c, t = 0) - \gamma_{eq}(c)$ increases with decreasing surfactant concentration. At the lowest concentration, $c =$ 0.0135 wt%, the initial interface tension is $\approx$35 mN m^{-1}. An even higher value may be expected for a surfactant-free water interface. The adsorption takes longer for smaller concentrations, decay rates decrease with smaller c. The early diffusive adsorption regime and intermediate plateaus of $\gamma(t)$ are not accessible with the current setup, they may be expected for $t < 10$ s.

When data of different runs of the experiment are compared, there appears to be a systematic deviation between sets of different days, whereas there is only little deviation between sets measured at the same day. We conclude that there are two error sources in the measurements: first, the uncertainty in the determination of the geometrical quantities, like the length and position of the contact line πd_{ring}, the angle of attack θ of the smectic film and the volume V_{air}, yield a relative statistical error of about 10% for the individual measurements and about 3% for the averaged values of γ_{eq}. On the other hand, there appears to be a systematic error on the order of 10% particularly for low surfactant concentrations, whose origin remains to be revealed. It could reflect the sensitivity of the experiment to small undocumented changes of environmental conditions.

It may be possible to produce bubbles at very low surfactant concentrations if the smectic film is drawn sufficiently slowly, so that the surfactant has time to adsorb to the surface. Then bubbles can be prepared at even lower concentrations than those reported above. Smectic bubbles at 0.005% SDBS concentration were prepared in our experiments, but they ruptured when the air bubble was inserted. Another liquid crystal, the commercial material 8CB (4-*n*-octyl-cyanobiphenyl) was also tested. Smectic A bubbles could be produced in surfactant solutions, but smectic A films are much more vulnerable to mechanical disturbances,[39] so that the air bubble impact leads to film rupture.

Finally, we note that the interface tension in smectics is an anisotropic quantity, *i.e.* it depends on the orientation of the mesogens at the surface. In our experiment, we measure the value for smectic layers parallel to the surface. Any other components are not accessible in this experiment. Anchoring energies of the director also represent an energy per surface area, but they are commonly orders of magnitude smaller than typical interface tensions of fluids, *cf. e.g.* ref. 40. They are not relevant here.

Summarizing, we have presented the first measurements of the dynamic surface tension of a liquid crystal towards a surfactant solution, employing a recently developed buoyancy method.[7] Interesting questions for further experiments with this system are the description and explanation of the details of the air bubble geometry (see Fig. 2), the use of other surfactants, including nonionic surfactants, and the study of other liquid crystalline materials. Polar liquid crystal materials might add interesting aspects. It is recommended to perform experiments in smectic C phases which develop films that are much less vulnerable to mechanical impacts than smectic A films. With a motor-controlled inflation/deflation technique it may be possible to study ratios of γ of freshly prepared films to the equilibrium γ_{eq} by controlled inflation or deflation of the smectic bubbles, even in absence of an air bubble. If an air bubble is inserted at an early time, a controlled liquid insertion rate and an appropriate consideration of the surface area increase might provide access to earlier adsorption stages. Such results could be comparable to others dynamic measurements (*e.g.* pending droplet studies by MacLeod and Radke[30]). A possible experiment is the inflation of a small smectic bubble, which is stalled until the surfactant coverage is equilibrated. Thereafter, the bubble is inflated to twice the size of the surface. If the initial bubble had roughly homogeneous thickness, one may expect that the lower hemisphere is then formed by a fresh film. A comparison of the mean curvatures of the top and bottom hemispheres (or, more exactly, sphere caps) of the smectic film will provide direct access to $\gamma(t = 0)/\gamma_{eq}$.

Acknowledgements

We are indebted to the German Aerospace Center, DLR, for financial support within project 50WM1430. L. S. and J. H. acknowledge support within the IRES student exchange project. Nattaporn Chattham is acknowledged for participating in some preparatory experiments.

References

1 A. Fernandez-Nieves, V. Vitelli, A. S. Utada, D. R. Link, M. Marquez, D. R. Nelson and D. A. Weitz, Novel defect structures in nematic liquid crystal shells, *Phys. Rev. Lett.*, 2007, **99**, 157801.

2 T. Lopez-Leon, A. Fernandez-Nieves, M. Nobili and C. Blanc, Nematic-smectic transition in spherical shells, *Phys. Rev. Lett.*, 2011, **106**, 247802.

3 H. L. Liang, J. Noh, R. Zentel, P. Rudquist and J. P. F. Lagerwall, Tuning the defect configurations in nematic and smectic liquid crystalline shells, *Philos. Trans. R. Soc., A*, 2013, **371**, 20120258.
4 A. Sengupta, C. Pieper, J. Enderlin, C. Bahr and S. Herminghaus, Flow of a nematogen pas a cylindrical micro-pillar, *Soft Matter*, 2013, **9**, 1937.
5 A. S. Utada, E. Lorenceau, D. R. Link, P. D. Kaplan, H. A. Stone and D. A. Weitz, Monodisperse double emulsions generated from a microcapillary device, *Science*, 2005, **308**, 5721.
6 Y. Iwashita, S. Herminghaus, R. Seemann and C. Bahr, Smectic membranes in aqueous environment, *Phys. Rev. E: Stat., Nonlinear, Soft Matter Phys.*, 2010, **81**, 051709.
7 K. Harth and R. Stannarius, Measurement of the interface tension of smectic membranes in water, *Phys. Chem. Chem. Phys.*, 2013, **15**, 7204–7209.
8 I.-H. Lin, D. S. Miller, P. J. Bertics, C. J. Murphy, J. J. de Pable and N. L. Abbott, Endotoxin-induced structural transformations in liquid crystalline droplets, *Science*, 2011, **332**, 1297.
9 T. Stoebe, P. Mach and C. C. Huang, Surface tension of free-standing liquid-crystal films, *Phys. Rev. E: Stat. Phys., Plasmas, Fluids, Relat. Interdiscip. Top.*, 1994, **49**(5), R3587.
10 P. Mach, S. Grantz, D. A. Debe, T. Stoebe and C. C. Huang, Surface tension of several liquid-crystal compounds in the smectic-A or smectic-Ad phase, *J. Phys. II*, 1995, **5**(2), 217.
11 B. Song and J. Springer, Surface phenomena of liquid crystalline substances: Temperature-dependence of surface tension, *Mol. Cryst. Liq. Cryst.*, 1997, **307**, 69.
12 P. Mach, C. C. Huang, T. Stoebe, E. D. Wedell, T. Nguyen, W. H. De Jeu, F. Guittard, J. Naciri, R. Shashidhar, N. Clark, I. M. Jiang, F. J. Kao, H. Liu and H. Nohira, Surface tension obtained from various smectic free-standing films: The molecular origin of surface tension, *Langmuir*, 1998, **14**(15), 4330.
13 H. Schüring, C. Thieme and R. Stannarius, Surface tensions of smectic liquid crystals, *Liq. Cryst.*, 2001, **28**, 241.
14 M. Tintaru, R. Moldovan, T. Beica and S. Frunza, Surface tension of some liquid crystals in the cyanobiphenyl series, *Liq. Cryst.*, 2001, 793.
15 J.-W. Kim, H. Kim, M. Lee and J. J. Magda, Interfacial tension of a nematic liquid crystal/water interface with homeotropic surface alignment, *Langmuir*, 2004, **20**, 8110–8113.
16 M. A. Gharbi, D. Sec, T. Lopez-Leon, M. Nobili, M. Ravnik, S. Zumer and C. Blanc, Microparticles confined to a nematic liquid crystal shell, *Soft Matter*, 2013, **9**, 6911.
17 J. E. Proust, E. Perez and L. Ter-Minassian-Saraga, Films minces de cristal liquide nematique sur support liquide structure, tensions superficielles et tension de ligne, *Colloid Polym. Sci.*, 1978, **256**, 666.
18 S. Dölle, K. Harth, T. John and R. Stannarius, Impact and embedding of picoliter droplets into freely suspended smectic films, *Langmuir*, 2014, **30**, 12712–12720.
19 A. E. Alexander, Interfacial tension, viscosity and potential changes produced by insoluble monolayers at the oil/water interface, *Trans. Faraday Soc.*, 1941, **37**, 117–119.
20 A. F. H. Ward and L. Tordai, Existence of time dependence for interfacial tensions of solutions, *Nature*, 1944, **154**, 146.
21 R. Miller and V. B. Fainerman, Surfactant adsorption layers at liquid–liquid interfaces, *Handbook of Surfaces and Interfaces of Materials*, Academic Press, London, Bristol, 2001, vol. 1, ch. 6, p. 383.
22 R. A. Campbell and C. D. Bain, External-reflection ft-ir spectroscopy of c10e8 at an expanding water surface, *Vib. Spectrosc.*, 2004, **35**, 205.
23 C. D. Bain, The overflowing cylinder sixty years on, *Adv. Colloid Interface Sci.*, 2008, **144**, 4–12.
24 R. A. Campbell, S. R. W. Parker, J. P. R. Day and C. D. Bain, External reflection ftir spectroscopy of the cationic surfactant hexadecyltrimethylammonium bromide (ctab) on an overflowing cylinder, *Langmuir*, 2004, **20**, 8740.
25 C. E. Morgan, C. J. W. Breward, I. M. Griffiths, P. D. Howell, J. Penfold, R. K. Thomas, I. Tucker, J. T. Petkov and J. R. P. Webster, Kinetics of surfactant desorption at an air–solution interface, *Langmuir*, 2012, **28**, 17339–17348.
26 Y. He, P. Yazhgur, A. Salonen and D. Langevin, Adsorption–desorption kinetics of surfactants at liquid surfaces, *Adv. Colloid Interface Sci*, 2015, **222**, 377–384.
27 A. Bonfillon, F. Sicoli and D. Langevin, Dynamic surface tension of ionic surfactant solutions, *J. Colloid Interface Sci.*, 1994, **168**, 497–504.
28 A. F. H. Ward and L. Tordai, Time dependence of boundary tensions of solutions, *J. Chem. Phys.*, 1946, **14**, 453–461.
29 H. Ritacco, D. Langevin, H. Diamant and D. Andelman, Dynamic surface tension of aqueous solutions of ionic surfactants: Role of electrostatics, *Langmuir*, 2011, **27**, 1009–1014.
30 C. A. MacLeod and C. J. Radke, Surfactant exchange kinetics at the air/water interface from the dynamic tension of growing liquid drops, *J. Colloid Interface Sci.*, 1994, **166**, 74–88.
31 H.-L. Liang, S. Schymura, P. Rudquist and J. Lagerwall, Nematic-smectic transition under confinement in liquid crystalline colloidal shells, *Phys. Rev. Lett.*, 2011, **106**, 247801.
32 H.-L. Liang, E. Enz, G. Scalia and J. Lagerwall, Liquid crystals in novel geometries prepared by microfluidics and electrospinning, *Mol. Cryst. Liq. Cryst.*, 2011, **549**, 69–77.
33 M. K. Kumar and P. Ghosh, Coalescence of air bubbles in aqueous solutions of ionic surfactants in presence of inorganic salt, *Trans. Inst. Chem. Eng., Part A*, 2006, **84**, 703–710.
34 S. K. Haitand, P. R. Majhi, A. Blume and S. P. Moulik, A critical assessment of micellization of sodium dodecyl benzene sulfonate (sdbs) and its interaction with poly(vinyl pyrrolidone) and hydrophobically modified polymers, jr 400 and lm 200, *J. Phys. Chem. B*, 2003, **107**, 3650–3658.
35 H.-L. Liang, R. Zentel, P. Rudquist and J. Lagerwall, Towards tunable defect arrangements in smectic liquid crystal shells utilizing the nematic–smectic transition in hybrid-aligned geometries, *Soft Matter*, 2012, **8**, 5443.
36 K. May, K. Harth, T. Trittel and R. Stannarius, Dynamics of freely floating smectic bubbles, *Europhys. Lett.*, 2012, **100**, 16003.

37 S. Trabelsi, J.-F. Argillier, C. Dalmazzone, A. Hutin, B. Bazin and D. Langevin, Effect of added surfactants in an enhanced alkaline/heavy oil system, *Energy Fuels*, 2011, **25**, 1681.
38 C. M. Phan, A. V. Nguyen and G. M. Evans, Dynamic adsorption of sodium dodecylbenzene sulphonate and dowfroth 250 onto the air–water interface, *Miner. Eng.*, 2005, **18**, 599–603.
39 K. May, K. Harth, T. Trittel and R. Stannarius, Freely floating smectic films, *ChemPhysChem*, 2014, **15**, 1508–1518.
40 U. Kühnau, A. G. Petrov, G. Klose and H. Schmiedel, Measurement of anchoring energy of a nematic liquid crystal, 4-cyano-4′-*n*-pentylbiphenyl, on langmuir-blodgett films of dipalmitol phosphatidycholine, *Phys. Rev. E: Stat., Nonlinear, Soft Matter Phys.*, 1999, **59**, 578.

